Electronic Supplementary Material (ESI) for ChemComm.

Supplementary information for

Drug orientations within statin-loaded lipoprotein nanoparticles by ^{19}F solid-state NMR

Sophie Lau, Naomi Stanhope, John Griffin, Eleri Hughes, David A. Middleton

Table of Contents

1. Methods and Materials

Expression of N-terminally His-tagged apoA-I was carried out by following previously published methods.[1] A pNFXex expression vector coding for human apoA-I with an N-terminal His tag (kindly provided by Dr M. Oda, Oakland Research Institute, USA) was transformed into E*. coli* BL21 (DE3) cells (Agilent Technologies) and grown at 37°C at 200 rpm in LB media containing 100 µg/ml ampicillin (Melford Laboratories Ltd) until the $OD_{600} \geq 0.6$. Protein expression was induced with the addition of 1 M IPTG (Melford Biolaboratories Ltd) to a final concentration of 1 mM, and incubated at 37^{o}C, at 200 rpm for 5 hours. The plasmid construct expresses apoA-I with an E2D mutation enabling removal of the His-tag by cleavage of the acid-labile Asp2-Pro3 peptide bond with formic acid, leaving the native residues 3-243. The cells were centrifuged at 5000 x g for 20 minutes. To lyse the cells, the pellet was resuspended in lysis buffer (6 M guanidine HCl, 20 mM $NaPO_4$, 0.5 M NaCl) pH 7.4, and frozen at -20^{o}C overnight. Before sonication of the cell lysate PMSF (200 mM stock) was added to a final concentration of 1 mM. To further lyse the cells, the sample was sonicated for 5 cycles on ice, with intervals of 15 seconds on and 60 seconds off at an amplitude of 22 microns. The cell debris was removed by centrifugation at 43 000 x g for 30 minutes at 4°C.

His-trap chromatography using an ÄKTA Start chromatography system and UNICORN Start 1.0 software (GE Healthcare) was used to purify the fusion protein. The 5 ml HisTrap FF pre-packed nickel Sepharose column (GE Healthcare) was washed with dH_2O and equilibrated with lysis buffer pH 7.4, at a flow rate of 5 ml/min. The lysate was diluted with an equal volume of lysis buffer pH 7.4 before loading onto the column at the flow rate of 5 ml/min, and 10 ml fractions were collected. The column was washed in succession with lysis buffer pH 7.4, and 20 mM $NaPO_4$ and 0.5 M NaCl containing an increasing concentration of imidazole to wash non-specific binding proteins (20 mM and 45 mM imidazole) and elute the apoA-I fusion protein (500 mM imidazole). Fractions containing the fusion protein were dialysed (12 - 14 kDa MWCO tubing) overnight in dialysis buffer pH 7.4 (50 mM Tris-HCl, 1 mM EDTA, 1 mM benzamidine hydrochloride) at 4°C.

Formic acid 45% (v/v) was added to the fusion protein and the solution was heated at 55°C for 5 h. To separate the cleaved his-tag and the apoA-I protein, the solution was dialysed in 5 L of dialysis buffer pH 8.0 overnight twice, at 4°C with 1

buffer change. After dialysis the concentration of apoA-I was measured using the Nanodrop 2000 (Thermo Scientific) and stored at -20^{o}C until use.

1.2. Production of rHDL particles: The widely established detergent mediated sodium cholate dialysis method was used in the production of rHDL particles.[2] POPC (Avanti®) and fluvastatin or rosuvastatin were dissolved in chloroform: methanol 1:1 (v/v) to a final molar ratio of 1: 20 (M/M) statin: POPC and dried with N_2 to form a thin film. All samples were prepared in rHDL buffer (10mM Tris base, 1mM EDTA, 1mM NaN_3) pH 7.4. The lipid/statin only samples were resuspended in rHDL buffer to form MLVs and analysed by NMR directly without the addition of sodium cholate. The lipid/statin films for the rHDL samples were resuspended with rHDL buffer containing sodium cholate (30 mg/ml stock) to a final lipid: detergent molar ratio of 1:1 (M/M). The solution was incubated for 2 hours at 4°C with stirring until clear. ApoA-I was added to the POPC/detergent mixture at a protein: lipid molar ratio of 1:100 (M/M) and incubated overnight at 4°C. Samples were transferred to dialysis tubing (12 - 14 kDa MWCO) and dialysed against buffer to remove the sodium cholate. A total of 5 buffer changes were carried out each in 2L of buffer to ensure a 500-fold excess over at least 3 days.

1.3. Flotation ultracentrifugation of rHDL: Flotation ultracentrifugation was used to separate lipid-free apoA-I and the rHDL particles. The method was adapted from protocols used to separate plasma lipoproteins and heterogenous rHDL particles.**[2-4]** To increase the rHDL sample density to greater than 1.21 g/ml 1.5 ml of 38 % (w/v) NaBr was added to 0.5 ml of rHDL particles. In a 10.4 ml centrifuge tube (Beckman Coulter), the solutions were under-layered in the tube (top to bottom), 0.5 ml of rHDL buffer, 7.9 ml of 1.21 g/ml density NaBr solution, and 2.0 ml of sample. The samples were centrifuged at 65,000 rpm for 22 hours at 4°C in a type 70.1 Ti rotor (Beckman Coulter). After centrifugation five 0.5 ml aliquots were collected from the top of the solution. The fractions were dialysed at 4^{o}C to remove the NaBr with at least two buffer changes over 2 days. The presence of rHDL particles in the fractions was confirmed by native gel electrophoresis. The sample concentrations were increased using an Amicon® Ultra-4 device with a 10,000 kDa MWCO (Merck). The spin concentrator was rinsed with dH_2O before the sample was centrifuged at 4000 x g for 30 minutes to reduce the sample volume for rHDL PEG precipitation.

1.4. PEG Precipitation of rHDL: For NMR analysis the rHDL samples were

precipitated using PEG.[5] PEG-6000 (40 % (w/v) stock) was added to the rHDL samples to a final concentration of 24 % (w/v). The samples were incubated at 4^{o}C and inverted to mix for at least 48 hours to ensure the sample precipitated. To pellet the precipitate and remove the supernatant, the samples (0.8 ml) were centrifuged at 41 krpm at 4°C for 2 hours in an SW 55 Ti rotor (Beckman Coulter). The PEG precipitated sample was stored at 4^{o}C until loaded into a 3.2 mm diameter magic-angle spinning rotor.

1.5. Analysis of rHDL size and structure: Non-denaturing gradient gel electrophoresis (NDGGE) was used to determine the homogeneity and size of the rHDL nanoparticles formed. The NDDGE gels were the 4-16% NativePAGE Bis-Tris protein gels (Invitrogen) and the marker was the HMW calibration kit for native electrophoresis (Amersham, GE Healthcare).[4, 6] The marker and samples were prepared to contain a final concentration of 1x NativePAGE sample buffer (4x stock, Invitrogen) and loaded into separate wells in the gel. The gels were run at 150 V with NativePAGE anode and cathode running buffer (Invitrogen) in the Bolt Mini Gel Tank (Novex Life Technologies) until the dye front approached the end of the gel. The gels were stained for 1 hour using InstantBlue (Expedeon) stain and imaged with the Molecular Imager ChemiDoc XRS+ Imaging System and Image Lab 4.0 Software (Bio-Rad).

For TEM analysis the carbon-coated copper grids (Agar Scientific) were glow-discharged before 3 µL of rHDL sample was pipetted onto the grid (protein concentration approximately 0.25 mg/ml). After 2 minutes the excess sample was blotted with filter paper. Followed by x3 wash steps with 35 µL dH_2O drops on parafilm in quick succession, with blotting in between each step. The grid was negatively stained by inverting onto 3 drops of 2 % (w/v) uranyl acetate (UA) on parafilm in quick succession with 2 minutes on the last drop of UA, and the excess stain blotted after each drop. The sample grid was dried under a heat lamp before imaging. The materials and microscope used were provided at the Astbury Centre for Structural Molecular Biology at the University of Leeds. The sample grid was imaged using a FEI Tecnai T12 microscope with a 120 keV Lab6 electron source and a Gatan US4000/SP 4k x 4k CCD camera, at 98 k magnification. The images were processed using FIJI software.[7]

The solution state CD measurements were taken using the Module B nitrogen flushed end station at B23 Diamond Light Source Synchrotron, Oxford, UK. The control background sample of POPC (4 mM) small unilamellar vesicles in rHDL buffer was prepared using sonication just prior to CD measurement to avoid formation of MLVs and light scattering effects. The rHDL sample volume was 20 µL and the approximate apoA-I concentration was 1.1 mg/ml. The number of scans for each sample was 3 and the temperature was 23^{o}C. The wavelength range was 260 - 180 nm, with a wavelength increment of 1 nm, slit width of 1 mm, and an integration time of 0.5 sec. A QS 0.1 mm pathlength cylindrical cuvette (Hellma) was used for each measurement. For secondary structure element analysis the CDApps software was used (Diamond Light Source, B23) and the CONTINLL algorithm with the basis set SMP56, SP43 + 13 membrane proteins.[8]

1.6. Solid-state NMR: All measurements were carried out on a Bruker Avance 400 spectrometer with an 89 mm bore magnet at a magnetic field strength of 9.3 T and equipped with a Bruker 3.2 mm magic-angle spinning HFXY probehead tuned to the ^{1}H and ^{19}F Larmor frequencies. All spectra were obtained at 25°C under static, non-spinning conditions. The proton-decoupled ^{19}F spectra of solid statins were obtained with an initial 2.5 µs 90° pulse at the frequency of ^{1}H followed by 2 ms ramped cross-polarisation from ^{1}H to ^{19}F at a proton nutation frequency of 40 kHz followed by SPINAL-64 proton decoupling at a field of 83 kHz during signal acquisition. The proton-decoupled ^{19}F NMR spectra of the hydrated rHDL samples were obtained with direct excitation of ^{19}F using a 4.2 µs 90° pulse followed by SPINAL-64 proton decoupling[11] at a field of 20 kHz during signal acquisition and are the result of averaging 102,400 transients. The ^{31}P NMR spectrum was obtained with direct excitation using a 4.5 µs 90° pulse with 20 kHz proton decoupling and is the result of averaging 32,000 transients. The proton-coupled ^{19}F NMR spectra of the rHDL samples were acquired under the same conditions except for omitting proton irradiation. The CP-MAS ^{15}N NMR spectrum of rHDL^{15}N-labelled apoA-I was obtained with 8 kHz magic-angle spinning. Hartmann-Hahn cross polarization was attained at a ^{1}H nutation frequency of 63 kHz and 2 ms contact time and followed by 80 kHz proton decoupling. The 2D ^{1}H-^{1}H NOESY experiment was carried out with 5 kHz MAS using the basic $\pi/2$-t_1-$\pi/2$-t_m-$\pi/2$ pulse sequence with a mixing time t_m of 500 ms, t_1 = 1024 increments in the indirect dimension and 32 transients averaged per increment.

The States-TPPI method was used for phase sensitive acquisition.

1.7. DFT calculations: Optimisation of the statin molecular geometry and calculation of the NMR parameters was performed using the CASTEP density functional theory code,[9] employing the GIPAW algorithm,[10] which allows the reconstruction of the all-electron wave function in the presence of a magnetic field. The CASTEP calculations employed the generalised gradient approximation (GGA) PBE functional[11] and core–valence interactions were described by ultrasoft pseudopotentials.[12] Geometry optimisations and NMR calculations were performed by placing the molecule in a 25 Å x 15 Å x 10 Å cell (atorvastatin) and in a 20 Å x 13 Å x 10 Å cell (fluva- and rosuvastatin). In the geometry optimisations the unit cell parameters were fixed and all atomic positions were allowed to vary. Both the geometry optimisation and NMR calculations were carried out with a planewave energy cut-off of 50 Ry and a single k-point at the fractional coordinate (0.25, 0.25, 0.25) in reciprocal space for integration over the Brillouin zone. The calculations generate the absolute shielding tensor ($\boldsymbol{\sigma}$) and diagonalisation of the symmetric part of $\boldsymbol{\sigma}$ yields as eigenvalues the principal components σ_{XX}, σ_{YY} and σ_{ZZ} and their orientations in the molecular frame are given by the eigenvectors. A ^{19}F shielding reference of 140.3 ppm determined from previous work was used.[13]

1.8. Computer simulations of NMR data: Calculations of dynamically-averaged ^{19}F chemical shift anisotropy $\Delta\delta_{av}$ and ^{1}H-^{19}F dipolar coupling d_{av} values as a function of angles α and β (defined in the main text) were performed using C programmes written specifically for the purpose.

Initial numerical calculations of $\Delta\delta_{av}$ took into account (i) the rotation of the molecule about a principal rotation axis that is parallel with the lipid bilayer normal and (ii) internal rotation of the fluorophenyl ring about the C-C bond. Lateral diffusion of the molecule within the lipid bilayer was not considered to be an influence on the measured parameters and so was disregarded. An initial state was set up in which the principal rotation axis and bilayer normal were coincident with the direction of B_0. The atomic coordinates of the statin molecules, taken from PDB files 1HWI (fluvastatin) and 1HWL (rosuvastatin), adjusted so that ^{19}F was at the origin, were rotated by angles α and β, which define the orientation of the ^{19}F chemical shift tensor components relative to the principal axis of molecular rotation. Unit vectors, δ_{11}, δ_{22}, δ_{33},

representing the directions of the three ^{19}F chemical shift tensor components, δ_{11}, δ_{22} and δ_{33}, in the molecular frame were also rotated by angles α and β. The directions of $\hat{\delta}_{11}$, $\hat{\delta}_{22}$ and $\hat{\delta}_{33}$, relative to the atomic coordinates of the statin were predicted using DFT as described above and as shown in Figure S1.

To simulate molecular motion the molecular (and vector) coordinates were rotated through 360° about the principal rotational axis in 30° increments and the aromatic ring was rotated through 360° in 30° increments after each molecular rotation about the principal axis. This value is consistent with values for other small molecules within lipid bilayers. The full rotational trajectory of the statin molecule, from the initial state, thus comprised 144 molecular orientations. For each molecular orientation the chemical shift was calculated from the atomic and vector coordinates using the equation

$$\delta_{av} = \delta_{11} sin^2\psi cos^2\phi + \delta_{22} sin^2\psi sin^2\phi + \delta_{33} cos^2\psi \qquad [1]$$

where δ_{11}, δ_{22} and δ_{33} are were measured from the powder spectra of the solid statins (Table 1) and ϕ and ψ are the angles defining the orientation of the ^{19}F chemical shift tensor components δ_{11} and δ_{33} relative to B_0. Angle ψ is the angle formed by $\hat{\delta}_{33}$ and the B_0 axis and angle ϕ is the angle between $\hat{\delta}_{11}$ and the plane formed by the B_0 axis, $\hat{\delta}_{33}$ and the origin. An order parameter S_{mol} of 1.0 was initially assumed (i.e., no excursions of the molecules away from the principal rotation axis were included in the simulations) and so $\Delta\delta_{av}$ for each α, β combination assumes the highest possible value when internal rotation of the fluorophenyl ring is considered. By introducing additional motional excursions of the molecules away from the principal axis into the simulation procedure, which in effect reduces S_{mol}, the values of $\Delta\delta_{av}$ as a function of α, β will decrease. This was not done, however, when it became apparent that even when S_{mol} = 1.0 the highest possible values $\Delta\delta_{av}$ were lower than the experimental values and so rotational of the fluorophenyl ring could be ruled out. The averaged chemical shift anisotropy value is given by

$$\Delta\delta_{av} = 0.667(\delta_{90} - \delta_0) \qquad [2]$$

where δ_0 is the motionally-averaged chemical shift when the principal rotation axis is parallel with B_0 (i.e., as in the initial condition above) and δ_{90} is when the

principal rotational axis is perpendicular to B_0.

A second computational routine was written to calculate $\Delta\delta_{av}$ and d_{av} as a function of α, β and S_{mol} in the absence of internal motion. $\Delta\delta_{av}$, is given by[14-15]

$$\Delta\delta_{av} = 0.5S_{mol}\Delta\delta_{st}(3cos^2\beta - 1 - \eta sin^2\beta cos2\alpha) \quad [3]$$

where η is the chemical shift asymmetry parameter and $\Delta\delta_{st}$ the static chemical shift anisotropy measured from the powder spectra of the solid statins (Table S1). The four ^{1}H-^{19}F dipolar coupling values were calculated from the atomic coordinates of the fluorine and four neighbouring protons in the fluorophenyl ring after performing rotations by α and β. Each of the four coupling values were calculated using the equation

$$d_{av} = d_{st}S_{mol}3(cos^2\theta - 1)/2 \quad [4]$$

where d_{st} is the static dipolar coupling constant and θ is the angle between each ^{1}H-^{19}F dipolar vector and the principal rotation axis. Matrices of $\Delta\delta_{av}$ and d_{av} values were obtained by varying α and β from 0° to 180° in 0.1° increments, and those values of α and β giving $\Delta\delta_{av}$ within ±5 % of the measured $\Delta\delta_{av}$ value were recorded. The procedure was repeated for S_{mol} = 1.0 and S_{mol} = 0.5 to place upper and lower limits on α and β within realistic bounds. Finally, the values of $\Delta\delta_{av}$ and d_{av} for each of the recorded [α, β] pairs were used to simulate proton-coupled ^{19}F NMR spectra using the SIMPSON platform, which were compared with the experimental spectra to find the closest agreement..

Tables

Table S1. Experimental and calculated static chemical shift parameters for solid statins. The convention $|\delta_{11} - \delta_{iso}| > |\delta_{33} - \sigma_{iso}| > |\delta_{22} - \delta_{iso}|$ is followed, with $\delta_{iso} = (\delta_{11} + \delta_{22} + \delta_{33})/3$. The reduced anisotropy $\Delta\delta = \delta_{11} - \delta_{iso}$ and asymmetry parameter $\eta = (\delta_{22} - \delta_{33})/\Delta\delta$.

	δ_{11} (ppm)	δ_{22} (ppm)	δ_{33} (ppm)	δ_{iso} (ppm)	$\Delta\delta$ (ppm)	η
Fluvastatin exp.	-57.07	-125.61	-166.31	-116.33	59.26	0.69
Fluvastatin calc.	-40.92	-145.46	-188.97	-125.11	84.20	0.52
Rosuvastatin exp.	-50.21	-121.86	-163.60	-111.89	61.88	0.68
Rosuvastatin calc.	-29.18	-130.90	-191.12	-117.07	87.89	0.69

Table S2. Experimental dynamically-averaged chemical shift parameters for fluvastatin and rosuvastatin in rHDL and DOPC multilamellar vesicles.

	δ_{11}(av) (ppm)	δ_{22} (av) (ppm)	δ_{33} (av) (ppm)	δ_{iso} (av) (ppm)	$\Delta\delta$ (av) (ppm)	η (av)
Fluvastatin rHDL	-110.62	-119.87	-119.87	-116.78	6.16	0.00
Rosuvastatin rHDL	-103.29	-115.71	-115.71	-111.57	8.28	0.00
Fluvastatin DOPC (1)	-116.99	-116.99	-117.88	-116.99	-0.88	0.00
Fluvastatin DOPC (2)	-116.68	-112.45	-112.45	-116.68	4.23	0.00
Rosuvastatin DOPC (1)	-102.74	-115.88	-115.88	-111.50	8.76	0..00
Rosuvastatin DOPC (2)	-108.82	-108.12	-115.35	-111.00	-4.35	0.00

Table S3. Values of α and β determining the average orientation of fluvastatin and rosuvastatin in rHDL and pure POPC vesicles, determined from the combined analysis of dynamically-averaged ^{19}F chemical shift anisotropy and ^{1}H-^{19}F dipolar couplings. The notation (1) and (2) refers to the two components of the spectra observed when the statins are embedded in POPC vesicles. Errors in α of ± 5° and errors in β of ± 1.5° represent the upper and lower limits of the angles when S_{mol} = 1.0 and 0.5, respectively.

	Average orientation defined by [α, β]			
	A	B	C	D
Flu-rHDL	[5°, 45°]	[5°, 135°]	[175°, 45°]	[175°, 135°]
Ros-rHDL	[5°, 43°]	[0°, 137°]	[180°, 43°]	[180°, 137°]
Flu-DOPC (1)	[0°, 48°]	[0°, 132°]	[180°, 48°]	[180°, 132°]
Flu-DOPC (2)	[10°, 46°]	[10°, 134°]	[170°, 46°]	[170°, 134°]
Ros-DOPC (1)	[0°, 43°]	[0°, 137°]	[180°, 43°]	[180°, 137°]
Ros-DOPC (2)	[10°, 50°]	[10°, 130°]	[170°, 50°]	[170°, 130°]

Figures

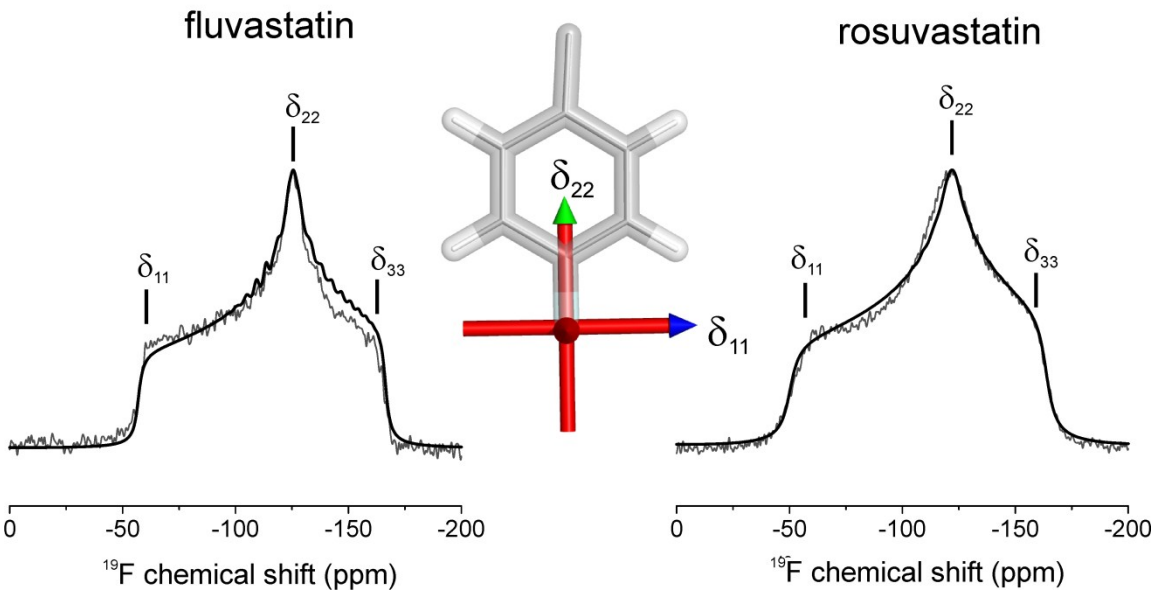

Figure S1. Static proton-decoupled ^{19}F solid-state NMR spectra of solid fluvastatin and rosuvastatin. Chemical shift components are taken from the line shapes of best fit, which were calculated by least-squares analysis using the Bruker Topspin routine Sola. According to DFT calculations, the ^{19}F chemical shift tensors are oriented with the least shielded principal component δ_{11} exactly in the plane of the aromatic ring and δ_{22} directed along the C-F bond, as is the case for other fluoroaromatic compounds.

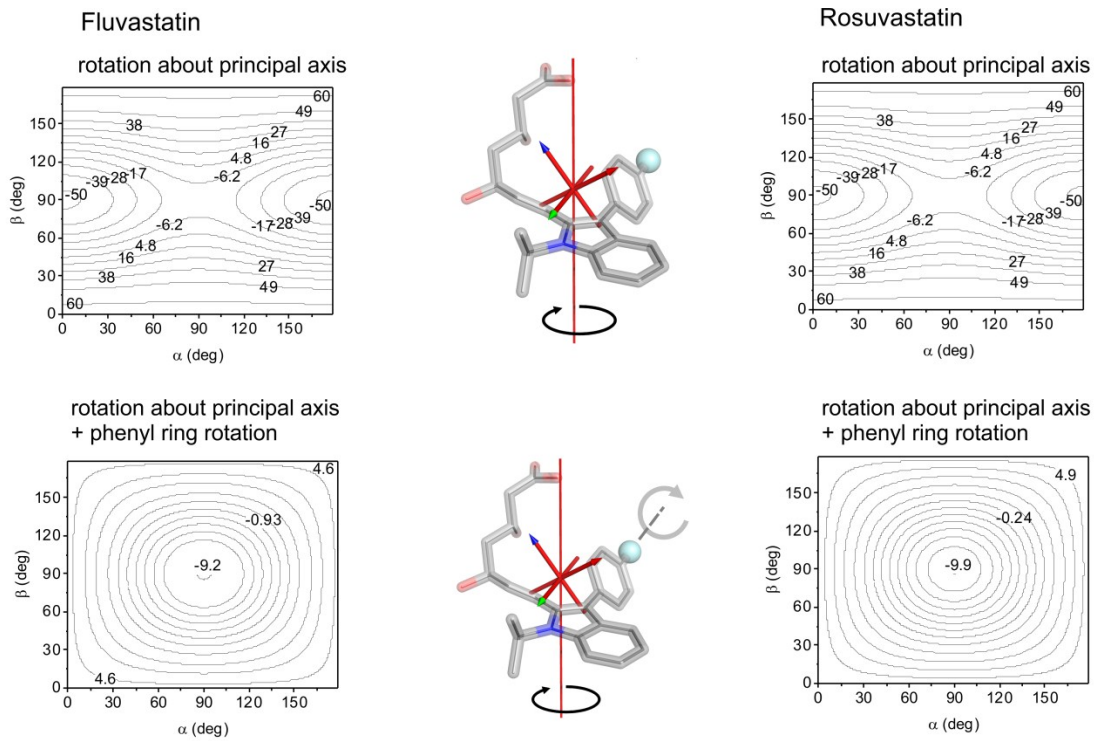

Figure S2. Calculated values of the dynamically-averaged anisotropy $\Delta\delta_{av}$ (in ppm) as a function of angles α and β. Left: values for fluvastatin undergoing rotation about a principal axis only (top), and with additional internal rotation of the fluoroaromatic ring (bottom), as indicated on the structures shown in the middle section. The upper and lower values of $\Delta\delta_{av}$ calculated for ring rotation (4.6 ppm and -9.2 ppm, respectively) are the maximum and minimum values possible. Right: values of $\Delta\delta_{av}$ for rosuvastatin calculated in the same way.

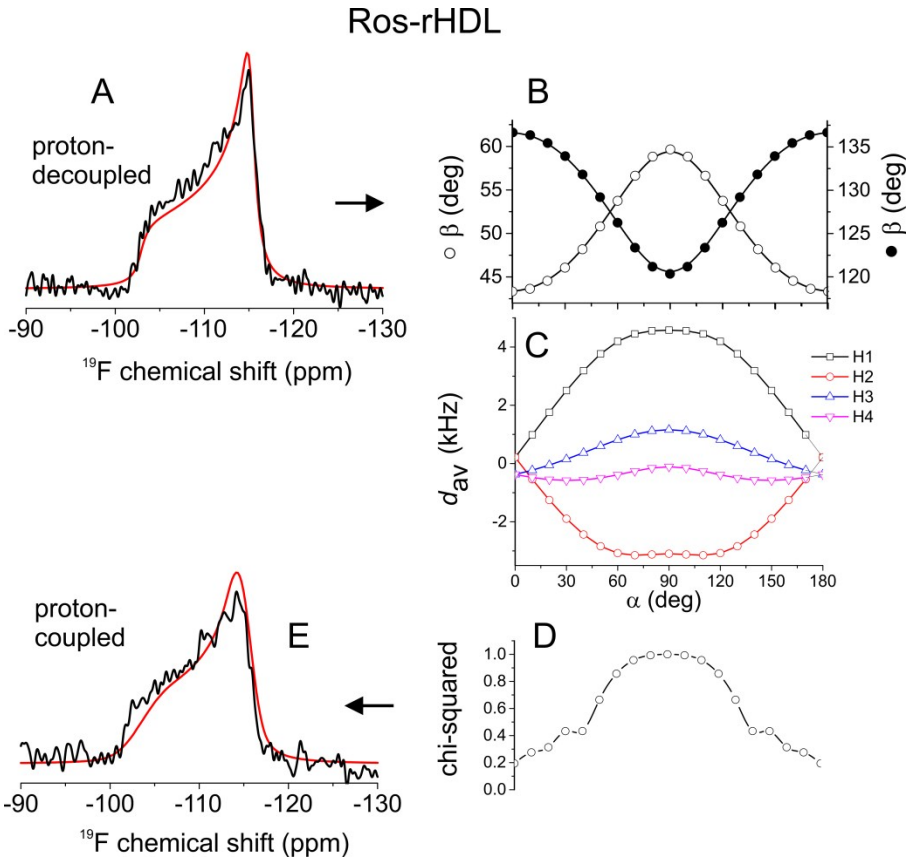

Figure S3. Analysis of the ^{19}F NMR spectra of rosuvastatin-loaded rHDL. A: The value of $\Delta\delta_{av}$ (8.28 ppm) was obtained from the proton-decoupled spectrum (black) by least-squares fitting of a simulated lineshape (red). B: $\Delta\delta_{av}$ is consistent with the pairs of α and β values shown by the lines. Discrete values of α (given in 10° increments) and corresponding β values denoted by the filled and open circles were used to simulate proton-coupled spectra as described below. C: Each of the discrete [α, β] pairs define a specific statin orientation relative to a principal axis of rotation. From each orientation were calculated four rotationally-averaged dipolar couplings between ^{19}F and the protons (H1-H4) in the fluorophenyl ring. D: Proton-coupled spectra were simulated for each [α, β] pair and the corresponding dipolar coupling values. Chi-squared values represent the agreement between each simulated spectrum and the experimental dipolar-coupled spectrum. Note that [α, β] and [α, 180° - β] give the same spectrum and so each chi-squared value represents two pairs of angles. E: The line of closest agreement with the proton-coupled spectrum (chi-squared minimum) corresponds to the [α, β] values given in Table S3

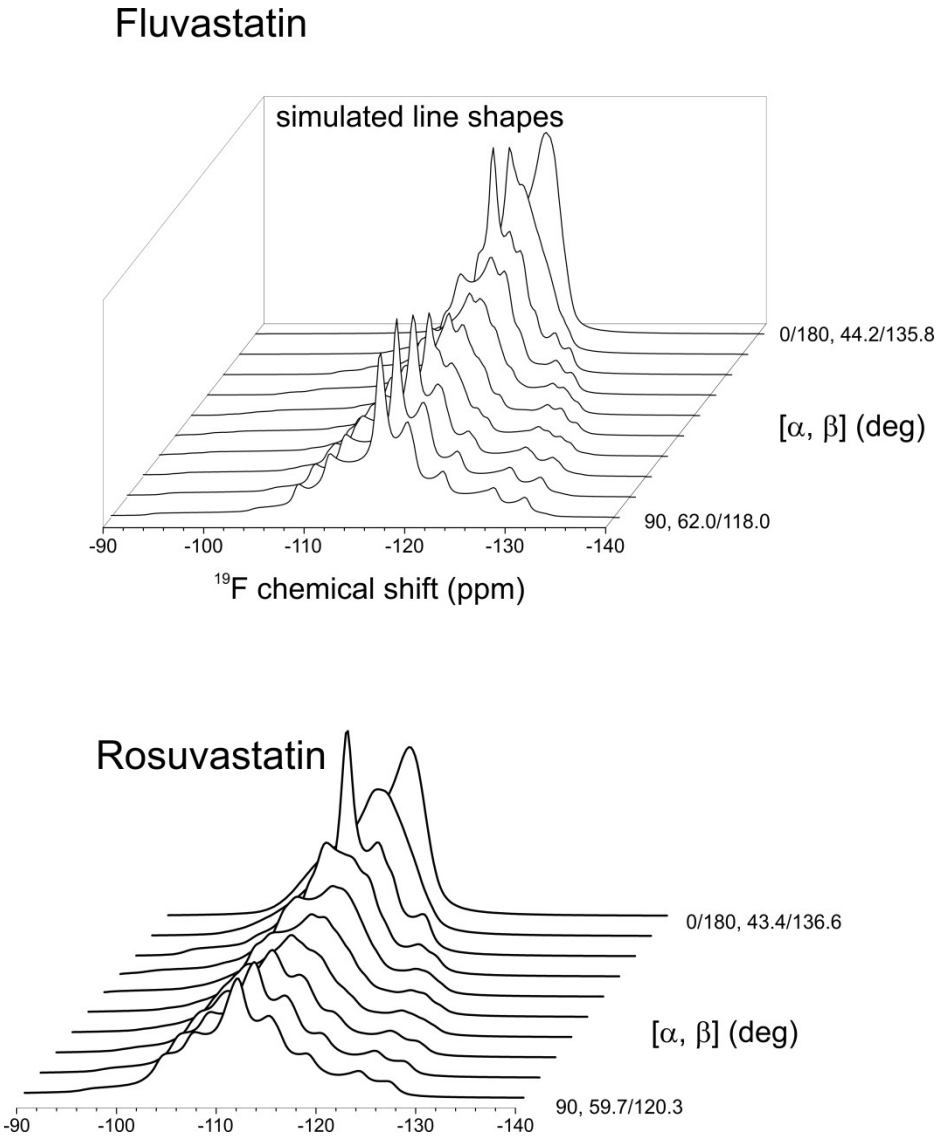

Figure S4. Simulated proton-coupled ^{19}F NMR line shapes for fluvastatin and rosuvastatin for values of α in 10° increments up to 90° and corresponding β values consistent with the measured values of $\Delta\delta_{av}$. Lineshapes for [α, β], [α, 180° - β], [180° - α] and [180° - α, 180° - β] are identical and hence the full range of lineshapes are represented.

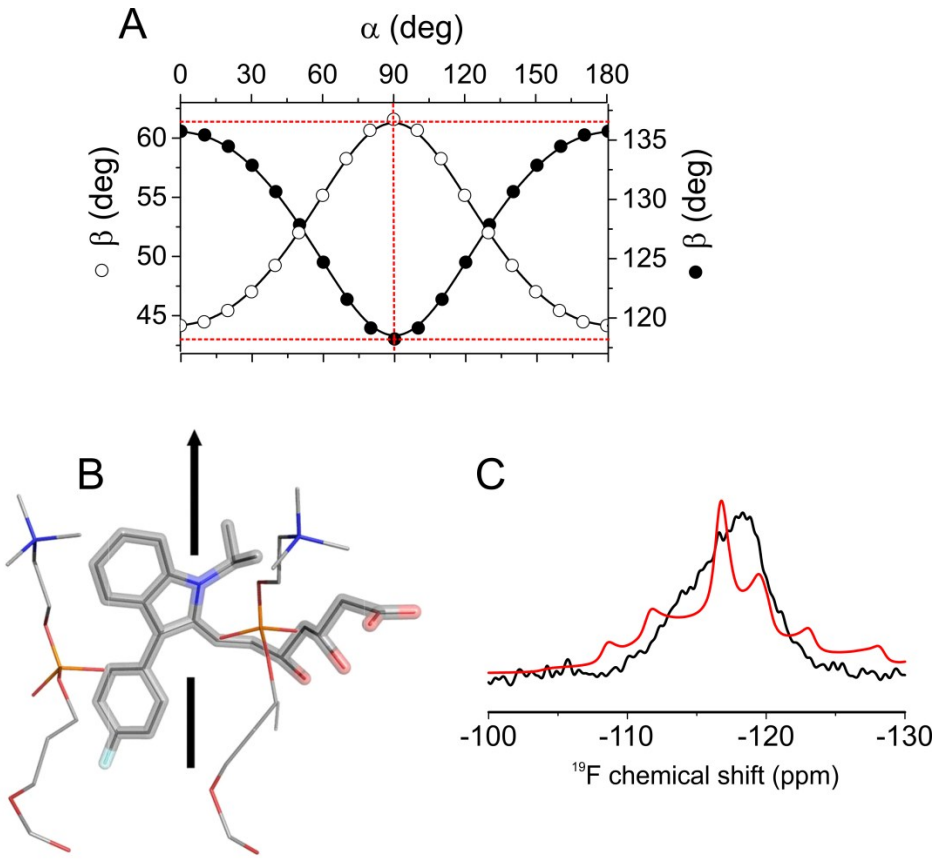

Figure S5. An alternative analysis of the data for fluvastatin embedded in rHDL bilayers. The [α, β] combination [90°, 62°], which is consistent with the measured $\Delta\delta_{av}$ value of 6.1 ppm (A), translates into a fluvastatin orientation in which the fluoroaromatic ring points toward the hydrophobic core or the bilayer (B). C: The simulated proton-coupled ^{19}F NMR line shape for this orientation (red; see also Fig. S4) agrees poorly with the experimental spectrum (black) and so this orientation is ruled out.

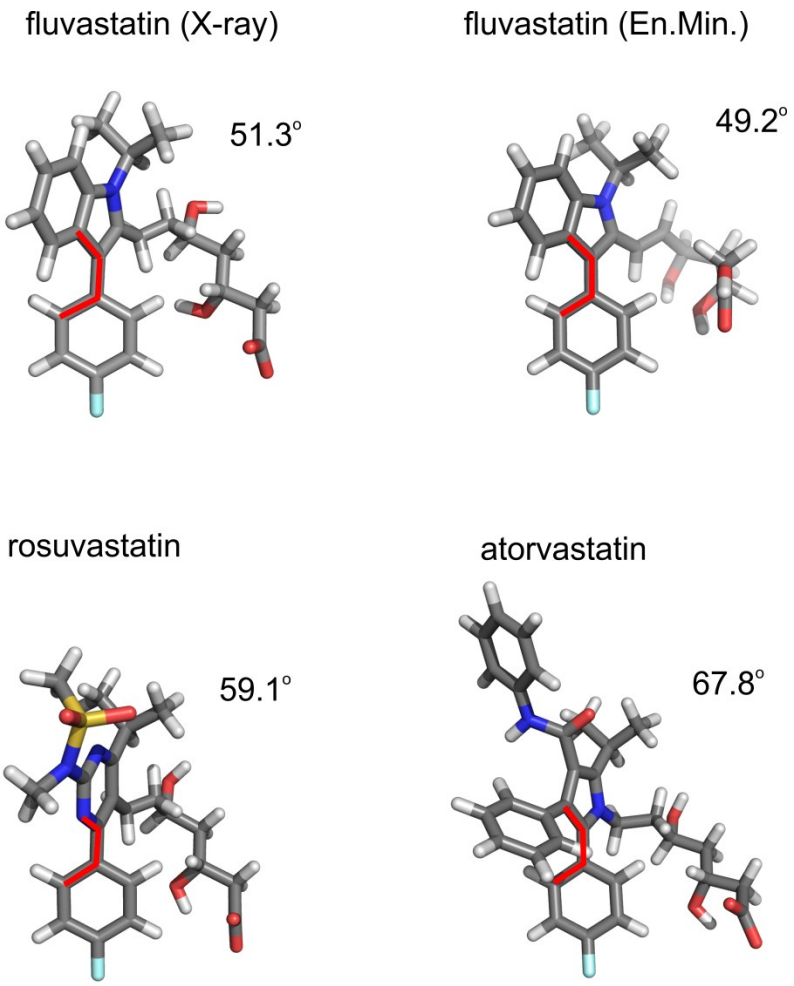

Figure S6. Molecular conformations of statins bound to human HMG-CoA reductase taken from the crystal structure in PDB file 1HWI (fluvastatin) and by energy minimisation of an *ab initio* structure of fluvastatin, and from PDB files 1HWL (rosuvastatin) and 1HWK (atorvastatin). The values given represent the torsion angle defining the out of plane orientation of the fluoroaromatic ring relative to the heteroaromatic ring.

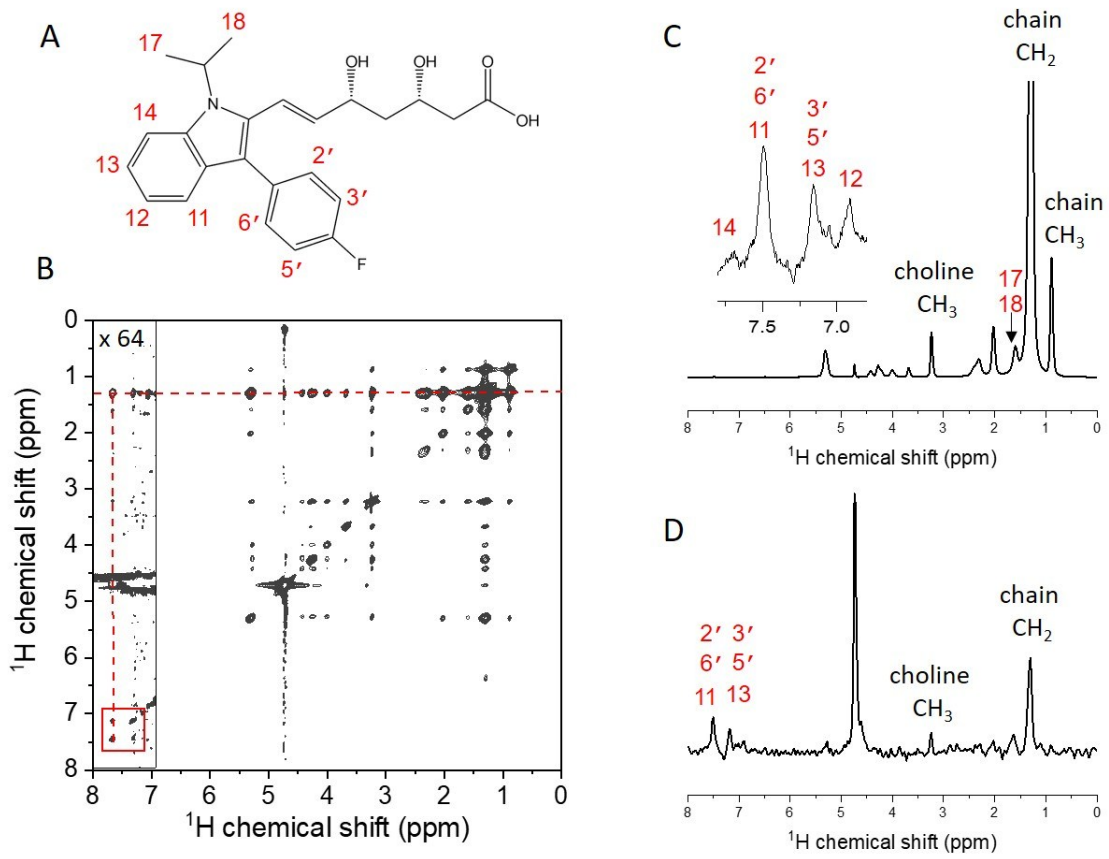

Figure S7. Depth of penetration of fluvastatin in POPC bilayers probed by ^{1}H-^{1}H NOESY NMR with magic-angle spinning at 5 kHz. A: Chemical structure of fluvastatin indicating the proton numbering scheme. B: NOESY spectrum of fluvastatin in POPC large multilamellar vesicle bilayers (lipid to drug molar ratio of 20:1). Cross-peaks in the aromatic region, where only drug resonances occur, indicate intermolecular NOE interactions between the drug aromatic protons and the lipid hydrocarbon chain protons at 1.3 ppm. The red box highlights the cross-peaks between 2'/6' and 3'/5'. C: Horizontal slice through the 2D spectrum at the position indicated. D: Vertical slice through the 2D spectrum, indicating the intermolecular NOE interactions between drug aromatic protons and lipid hydrocarbon and choline protons.

Additional references

1. Townsend, D.; Hughes, E.; Hussain, R.; Siligardi, G.; Baldock, S.; Madine, J.; Middleton, D. A., Heparin and Methionine Oxidation Promote the Formation of Apolipoprotein A-I Amyloid Comprising alpha-Helical and beta-Sheet Structures. *Biochemistry* **2017,** *56* (11), 1632-1644.
2. Jonas, A., *Methods in Enzymology* **1986,** *128*, 553-582.
3. Schumaker, V. N.; Puppione, D. L., SEQUENTIAL FLOTATION ULTRACENTRIFUGATION. *Methods in Enzymology* **1986,** *128*, 155-170.
4. Cavigiolio, G.; Shao, B.; Geier, E. G.; Ren, G.; Heinecke, J. W.; Oda, M. N., The interplay between size, morphology, stability, and functionality of high-density lipoprotein subclasses. *Biochemistry* **2008,** *47* (16), 4770-4779.
5. Mors, K.; Roos, C.; Scholz, F.; Wachtveitl, J.; Dotsch, V.; Bernhard, F.; Glaubitz, C., Modified lipid and protein dynamics in nanodiscs. *Biochimica Et Biophysica Acta-Biomembranes* **2013,** *1828* (4), 1222-1229.
6. Dalla-Riva, J.; Lagerstedt, J. O.; Petrlova, J., Structural and Functional Analysis of the ApolipoproteinA-I A164S Variant. *Plos One* **2015,** *10* (11).
7. Tinevez, J. Y.; Perry, N.; Schindelin, J.; Hoopes, G. M.; Reynolds, G. D.; Laplantine, E.; Bednarek, S. Y.; Shorte, S. L.; Eliceiri, K. W., TrackMate: An open and extensible platform for single-particle tracking. *Methods* **2017,** *115*, 80-90.
8. Hussain, R.; Benning, K.; Javorfi, T.; Longo, E.; Rudd, T. R.; Pulford, B.; Siligardi, G., CDApps: integrated software for experimental planning and data processing at beamline B23, Diamond Light Source. *Journal of Synchrotron Radiation* **2015,** *22*, 465-468.
9. Segall, M. D.; Lindan, P. J. D.; Probert, M. J.; Pickard, C. J.; Hasnip, P. J.; Clark, S. J.; Payne, M. C., First-principles simulation: ideas, illustrations and the CASTEP code. *Journal of Physics-Condensed Matter* **2002,** *14* (11), 2717-2744.
10. Pickard, C. J.; Mauri, F., All-electron magnetic response with pseudopotentials: NMR chemical shifts. *Physical Review B* **2001,** *63* (24).
11. Perdew, J. P.; Burke, K.; Ernzerhof, M., Generalized gradient approximation made simple. *Physical Review Letters* **1996,** *77* (18), 3865-3868.
12. Yates, J. R.; Pickard, C. J.; Mauri, F., Calculation of NMR chemical shifts for extended systems using ultrasoft pseudopotentials. *Physical Review B* **2007,** *76* (2).
13. Townsend, D.; Hughes, E.; Stewart, K. L.; Griffin, J. M.; Radford, S. E.; Middleton, D. A., Orientation of a Diagnostic Ligand Bound to Macroscopically Aligned Amyloid-beta Fibrils Determined by Solid-State NMR. *Journal of Physical Chemistry Letters* **2018,** *9* (22), 6611-6615.
14. Davis, J. H.; Auger, M., Static and magic angle spinning NMR of membrane peptides and proteins. *Progress in Nuclear Magnetic Resonance Spectroscopy* **1999,** *35* (1), 1-84.
15. Bechinger, B., The structure, dynamics and orientation of antimicrobial peptides in membranes by multidimensional solid-state NMR spectroscopy. *Biochimica Et Biophysica Acta-Biomembranes* **1999,** *1462* (1-2), 157-183.